Theoretical Analysis of the Elastomeric and Optical Properties of Networks of Semirigid Chains in the Swollen State

Yong Yang,† A. Kloczkowski, and J. E. Mark*

Department of Chemistry and The Polymer Research Center, University of Cincinnati, Cincinnati, Ohio 45221-0172

B. Erman and I. Bahar

Polymer Research Center and School of Engineering, Bogazici University, and TUBITAK Advanced Polymeric Materials Research Center, Bebek 80815, Istanbul, Turkey

Received May 16, 1994; Revised Manuscript Received March 30, 1995®

ABSTRACT: The recently proposed lattice model for segmental orientation in elongated networks of semirigid chains is used here to study the relationshipd among true stress, deformation, orientation, and birefringence. Of particular interest are the effects of the volume fraction of polymer (in a swollen lyotropic network) and the rigidity of the network chains (measured by the axial ratio of Kuhn segments of the chains) on stress–strain and stress–birefringence behavior. The elastomeric and optical behavior of the networks in isotropic and nematic states and networks undergoing phase transformation are thus characterized. Illustrative numerical analyses are also presented.

Introduction

Elastic and photoelastic properties of isotropic networks composed of flexible chains have long been well described in a number of theories.[1–5] These classic theories based on the flexible chain model assume that the elastic free energy of the deformed network is a sum of the elastic free energies of all chains and there intermolecular interactions are independent of deformation and can therefore be neglected. In this area, the phantom network model is a good approximation, at least to some extent, for real networks of flexible chains. Modern theories, such as the constrained-junction or the constrained-chain model, include contributions from intermolecular interactions from chain interpenetration and entanglements.[6–9] These theories have been successful in interpreting properties of isotropic networks of flexible chains but are deficient in describing properties of anisotropic networks and networks undergoing phase transformations under deformation.

Recently, there has been growing interest in other types of networks, most notably those obtained by cross-linking polymers that are semirigid chains.[10–42] Among these polymers are side-chain or main-chain polysiloxanes and polyacrylates,[12–31] cellulose derivatives,[32–36] and aromatic polyamides.[7,38] The unique structural feature of these networks is the hindrance to rotations about backbone bonds. This hindrance results from steric factors or from conjugated bonding, for example, the large rotational energy barriers for rigid units such as aromatic or cyclic rings and conjugated bonds. One of the characteristic features of these polymers is their natural tendency for self-alignment and formation of liquid-crystalline order in melt or in solution. As a result, such networks have unusual stress–strain and stress–optical birefringence properties. For example, experimental studies have demonstrated strongly nonlinear relationships among stress, strain, and birefringence.[16,39] These observations are incompatible with classical theories developed for networks of flexible chains. For these reasons, several theoretical approaches for networks of semirigid chains have been proposed and range from early phenomenological theories[40,41] to more recent molecular models.[26–31,44]

A critical review of existing data and results from experiments on lyotropic nematic elastomers indicates that two basic features of the semirigid chain have to be recognized in constructing a successful molecular theory. First, the degree of rigidity of the chains should appear as a parameter in the theory. Such a parameter may be introduced by assigning a length-to-width ratio, or axial ratio, for the Kuhn segments of the chains. Second, account should be taken of the effects of volume exclusion of the rigid Kuhn segments (which influences the entropy of packing of the chains). These two factors have, in fact, been incorporated in a lattice model for segmental orientation proposed recently by Erman *et al.*[29–31,44]

Phase transformation in a deformed, swollen network are of considerable interest, particularly because an isotropic–nematic transition may be driven by an external mechanical field or by changes in the concentration of the polymer. Such a network in the swollen state below the critical transition concentration c^* is isotropic, but the isotropic-to-nematic phase transformation may be brought about by macroscopic deformation. Sufficiently high degrees of swelling, however, may preclude the transition. On the other hand, in a dry or slightly swollen state the network may be nematic even in the absence of an external force if the axial ratio of the polymer's Kuhn segments is large enough.

In the present study, the lattice model of Erman *et al.* is used to study the relationship among stress, strain, degree of segmental orientation, and optical birefringence in networks having different degrees of swelling. The elastomeric and optical behaviors of the networks in isotopic and nematic states, and for networks undergoing phase transformation, are discussed, and illustrative results of numerical analyses of the model are presented.

Theory

In the theory of Erman, Bahar, Kloczkowski, and Mark,[29–31] the swollen network is assumed to consist

† Current address: Central Laboratories, Benjamin Moore and Co., Flanders, NJ 07836.

® Abstract published in *Advance ACS Abstracts,* May 15, 1995.

0024-9297/95/2228-4920$09.00/0

of n_2 cross-linked chains and n_1 solvent molecules. Each semirigid chain of the polymer network is modeled by a freely-jointed chain of m rigid rods (Kuhn segments), each having a specified length-to-width ratio x. The approach then uses the lattice model developed by Flory and refined by Flory and Ronca[42,43] to calculate the combinatorial and orientational contributions to the partition function and the Helmholtz free energy of the system. The main advantage of this lattice method is that it allows for continuous orientations of rods in the lattice, whereas in most lattice theories only discrete sets of orientations are allowed. By assuming the end-to-end vectors of the polymers chains transform affinely with deformation, and using the Lagrange multipliers method to calculate the orientational distribution function of polymer Kuhn segments, Erman *et al.* obtained the solution of this model. It is in the form of a set of three nonlinear equations with double integrals for Lagrange multipliers β, γ, and the mean disorientation index $\bar{y}$:

$$\frac{\bar{y}}{x} = \frac{1}{Z}\int_0^{2\pi} d\phi \int_0^{\pi} d\psi \sin\psi(|\sin\phi| + |\cos\phi|)f(\phi,\psi) \tag{1}$$

$$\frac{\lambda}{\sqrt{3m}} = \frac{1}{Z}\int_0^{2\pi} d\phi \int_0^{\pi} d\psi \cos\psi f(\phi,\psi) \tag{2}$$

$$\frac{\lambda}{\sqrt{3m\lambda v_2}} = \frac{1}{Z}\int_0^{2\pi} d\phi \int_0^{\pi} d\psi \sin\psi \cos\phi f(\phi,\psi) \tag{3}$$

where

$$Z = \int_0^{2\pi} d\phi \int_0^{\pi} d\psi f(\phi,\psi) \tag{4}$$

Here λ is the extension ratio defined as a ratio of the final length of the sample to the reference length, and v_2 is the volume fraction of polymer in the system. The mean disorientation index $\bar{y}$ is a measure of orientational ordering of the rods (Kuhn segments) and equals unity for an isotropic system and zero if all the rods are perfectly oriented along the preferred direction.

The orientation distribution function $f(\phi,\psi)$ is

$$f(\phi,\psi) = \sin\psi \exp[-ax \sin\psi(|\sin\phi| + |\cos\phi|) + \beta\cos\psi + \gamma \sin\psi(\cos\phi + \sin\phi)] \tag{5}$$

with

$$a \equiv -\ln[1 - v_2(1 - \bar{y}/x)] \tag{6}$$

The evaluation of β, γ, and $\bar{y}$ enables calculation of the stress and the orientation function S. This latter quantity is defined as

$$S = \frac{\int_0^{2\pi} d\phi \int_0^{\pi} d\psi\, P_2(\cos\psi) f(\phi,\psi)}{\int_0^{2\pi} d\phi \int_0^{\pi} d\psi\, f(\phi,\psi)} \tag{7}$$

where the orientational distribution function $f(\phi,\psi)$ defined by eq 5 is calculated by solving the system of eqs 1–6 for β, γ, and $\bar{y}$.

The true stress in uniaxial deformation σ (defined as the elastic force per unit of deformed area) is obtained from the elastic free energy ΔA_m by the relation:

$$\sigma = \frac{1}{V}\lambda\left(\frac{\partial \Delta A_m}{\partial \lambda}\right)_{T,V,n_1,n_2,(n_{j,k})_{eq}} \tag{8}$$

where V is the volume of the system, λ is the extension ratio, and the subscript $(n_{j,k})_{eq}$ specifies that the derivative is calculated for the equilibrium orientational distribution of Kuhn segments. The theory of Erman *et al.* leads to the following expression for the true stress:

$$\sigma = \frac{k_B T}{V} n_2 \left(\frac{m}{3}\right)^{1/2} \lambda[\beta - \gamma/(v_2\lambda^3)^{1/2}] \tag{9}$$

where T is the temperature and k_B the Boltzmann constant.

The stress–birefringence is characterized using Hermans' relation between the orientation function S and the polarizability of the chain:[45]

$$S = \frac{\overline{\Delta\alpha}}{\alpha_{\parallel} - \alpha_{\perp}} = \frac{3\,\overline{\cos^2\psi} - 1}{2} \tag{10}$$

where $\alpha_{\parallel}$ and $\alpha_{\perp}$ are the polarizabilities of the Kuhn segments in the direction parallel and perpendicular to the Kuhn segment axis, respectively. The quantity $\overline{\Delta\alpha}$ is the mean difference (per Kuhn segment) between polarizabilities of a chain in directions parallel and orthogonal to the end-to-end vector. The polarizability of the chain is related to the refractive index n by the Lorentz–Lorenz equation:

$$\frac{n^2 - 1}{n^2 + 2} = \frac{4\pi}{3}\frac{\nu}{V}\bar{\alpha} \tag{11}$$

where ν is the number of chains in volume V. For a uniaxially deformed sample, the Lorentz–Lorenz relation is valid for two refractive indices, the one parallel (n_1) and the other perpendicular (n_2) to the direction of the strain:[46]

$$\frac{n_1^2 - 1}{n_1^2 + 2} = \frac{4\pi}{3}\frac{\nu}{V}\bar{\alpha}_{\parallel} \tag{12}$$

$$\frac{n_2^2 - 1}{n_2^2 + 2} = \frac{4\pi}{3}\frac{\nu}{V}\bar{\alpha}_{\perp} \tag{13}$$

If $\Delta n = n_1 - n_2 \ll n$, then

$$\frac{n_1^2 - 1}{n_1^2 + 2} - \frac{n_2^2 - 1}{n_2^2 + 2} \approx \frac{6\bar{n}}{(\bar{n}^2 + 2)}\Delta n = \frac{4\pi}{3}\frac{\nu}{V}\overline{\Delta\alpha} \tag{14}$$

and

$$\Delta n = \frac{(\bar{n}^2 + 2)^2}{n}\frac{2\pi}{9}\frac{\nu}{V}\overline{\Delta\alpha} \tag{15}$$

where

$$\bar{n} = \frac{n_1 + n_2}{2} \tag{16}$$

is the mean refractive index.

For a perfectly oriented chain with the two refractive indices parallel and vertical to the chain designated as $n_{\parallel}^0$ and $n_{\perp}^0$, respectively

$$\Delta n_0 = n_{\parallel}^{0} - n_{\perp}^{0} = \frac{2\pi(\bar{n}^2+2)^2}{9\bar{n}}\frac{\nu}{V}(\alpha_{\parallel}-\alpha_{\perp}) \quad (17)$$

where Δn_0 is the intrinsic birefringence of the chain. Combining eqs 15 and 17 gives for the relationship between birefringence and orientation function S:

$$S = \frac{\overline{\Delta\alpha}}{\alpha_{\parallel}-\alpha_{\perp}} = \frac{\Delta n}{\Delta n_0} \quad (18)$$

The birefringence for a uniaxially-deformed network is defined as the difference in refractive indices in directions parallel and perpendicular to the stretching direction. Corresponding, the strain–birefringence relationship for affine deformation is[5]

$$\Delta n = \left(\frac{2\pi\nu}{27V}\right)\left[\frac{(\bar{n}^2+2)^2\Gamma_2}{\bar{n}}\right](\alpha_e^{\,2}-\alpha_e^{\,-1})\left(\frac{V}{V_0}\right)^{2/3} \quad (19)$$

where α_e is the elongation ratio (and should not be confused with the polarizability α), V_0 is the volume of the network at the state of formation, and the coefficient Γ_2 is defined as

$$\Gamma_2 = \left(\frac{9}{10}\right)\sum_i \langle \mathbf{r}^{\mathrm{T}}\hat{\alpha}_i\mathbf{r}\rangle/\langle r^2\rangle_0 \quad (20)$$

Here, $\mathbf{r}^{\mathrm{T}}$ is the transpose of the end-to-end vector $\mathbf{r}$, and $\hat{\alpha}_i$ is the traceless tensor representing the anisotropy of the polarizability of the structural unit. The summation is over all structural units contributing to the birefringence, assuming the additivity of group polarizabilities. The reduced birefringence $[\Delta n]$ is defined (analogously to the reduced stress) as

$$[\Delta n] = \frac{\Delta n}{\alpha_e-\alpha_e^{-2}}\left(\frac{V}{V_0}\right)^{-1/3} \quad (21)$$

and for the affine chain model is independent of elongation. The stress-optical relation is given by

$$\Delta n = \left(\frac{2\pi}{27k_BT}\right)\left[\frac{(\bar{n}^2+2)^2\Gamma_2}{\bar{n}}\right]\sigma \quad (22)$$

where σ is the true stress defined as the elastic force per unit cross-sectional area of the deformed sample and k_B is the Boltzmann constant. The stress-optical coefficient C defined as

$$C \equiv \frac{\Delta n}{\sigma} = \frac{2\pi\Gamma_2(\bar{n}^2+2)^2}{27\bar{n}k_BT} \quad (23)$$

is a function of temperature T only for the affine network model and does not depend on the elongation.

Isotropic-to-Nematic Phase Transitions in the Deformed Swollen Networks

The phase adopted by a deformed swollen network is determined by the free energy of the network, which is a function of parameters such as the extension ratio α_e, applied force f, and volume fraction of polymer v_2. Thermodynamic parameters which are the easiest to control during the phase transformation are the length of the sample L (measured by the extension ratio α_e) and the applied force or load f. The isotropic–nematic phase transformation occurs at constant length (strain) when the Helmholtz elastic free energies ΔA_m in the nematic and the isotropic phases are equal:

$$\Delta A_m(\text{isotropic}) = \Delta A_m(\text{nematic}) \quad (24)$$

One may also study phase transformations at constant force, while the length of the sample changes. The proper free energy for studying these phase transformations is Gibbs free energy ΔG_m, which is the Legendre transform of ΔA_m:

$$\Delta G_m = \Delta A_m - fL \quad (25)$$

The phase transformation at constant force occurs when the Gibbs free energies of both phases are equal:

$$\Delta G_m(\text{isotropic}) = \Delta G_m(\text{nematic}) \quad (26)$$

It is also possible to study the phase transformation at constant stress, although the experimental adjustments required to give this constancy during a phase transformation are difficult.

The true stress σ is frequently used for the studies of strain–birefringence. The free energy for the study of the phase transformation at constant stress is

$$\Delta F_m = \Delta A_m - V\sigma \ln\lambda \quad (27)$$

and the criterion for phase transition at constant stress is therefore

$$\Delta F_m(\text{isotropic}) = \Delta F_m(\text{nematic}) \quad (28)$$

Numerical Analyses

Numerical analyses of the lattice model were carried out to study quantitatively the elastic and photoelastic properties, orientation, and phase transitions described above. The calculations were performed by first solving eqs 1–3 to obtain the exact numerical solutions for the unknown parameters β, γ, and $\bar{y}$ and then using these parameters to calculate the stress, orientation parameter, and birefringence as a function of strain. Details of the numerical method are described elsewhere.[44]

The calculations were done on an IBM 7171 mainframe computer, using two IMSL subroutines for double integration (DMLIN) and for solving sets of nonlinear equations (ZSPOW).

Results and Discussion

Figure 1 shows the numerical solution of the three nonlinear equations (eqs 1–3). The reduced mean disorientation index $\bar{y}/x$ is plotted against the axial ratio of the Kuhn segments x. The calculations were performed for network chains having $m = 100$ Kuhn segments between cross-links and for several values of the volume fraction of polymer v_2. The upper parts of the curves with large values of the reduced mean disorientation index $\bar{y}/x$ correspond to the isotropic state, and the lower parts with small $\bar{y}/x$ represent the nematic-phase solutions. The middle parts of the curves with positive slopes correspond to metastable regions. The phase transition may occur for a chain with specific x only when there are two $\bar{y}/x$ solutions in the isotropic and in the nematic region. The isotropic–nematic phase transformation for a chain with specified axial ratio x will occur at the volume fraction of the polymer v_2 (or at the extension ratio α_e) at which the appropriate free energies of the isotropic and the nematic solutions of eqs 1–3 are equal.

The curves in Figure 1 move toward smaller values of x with an increase in the deformation and volume fraction of the polymer, suggesting that a larger exten-

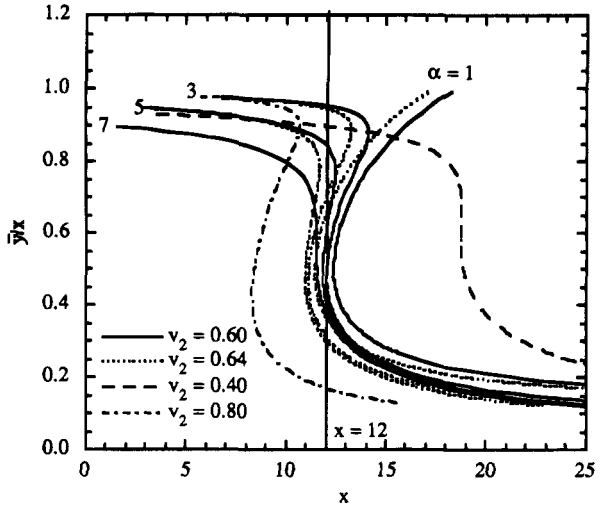

Figure 1. Mean reduced disorientation index $\bar{y}/x$ obtained from the solution of eqs 1–3 as a function of the axial ratio x of Kuhn segments (for chains composed of $m = 100$ Kuhn segments). The results are shown for several values of the extension ratio α_e and the volume fraction of the polymer v_2.

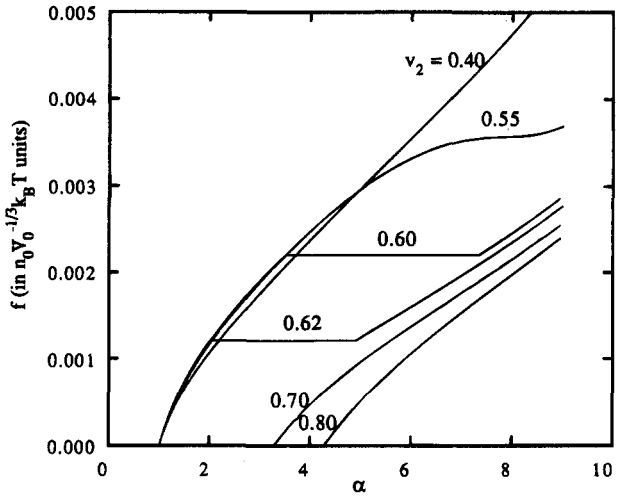

Figure 2. Force f versus extension ratio α_e for a swollen network undergoing phase transition at constant force. In this and the following figures, $x = 12$ and $m = 100$.

sion ratio is required to induce an isotropic-to-nematic phase transition at smaller v_2. For a swollen network with $x = 12$, $m = 100$, and $v_2 = 0.60$, the phase transition takes place at α_e larger than 3. Such a transition for the same network with a v_2 of 0.64 will occur at an α_e as small as 2. For a network with high v_2 (0.80), only one $\bar{y}/x$ solution on the nematic branch is found even for α_e less than 1.1, which means that for $x = 12$ the nematic phase is formed even in the undeformed network. For low v_2 (0.40), however, one $\bar{y}/x$ solution is observed corresponding to the isotropic state, and the nematic solution does not exist within the range of extensions considered.

Figures 2 and 3 show the elastic force f as a function of the extension ratio α_e. It was calculated for different values of v_2 for a network having $m = 100$ and $x = 12$ and undergoing phase transition either at constant force (Figure 2) or at constant length (Figure 3). Networks with v_2 around 0.60 show discontinuities due to the isotropic-to-nematic phase transformation. With increasing values of v_2, phase transformations are observed at lower extension ratios α_e. The phase transition does not occur for the polymer network with v_2

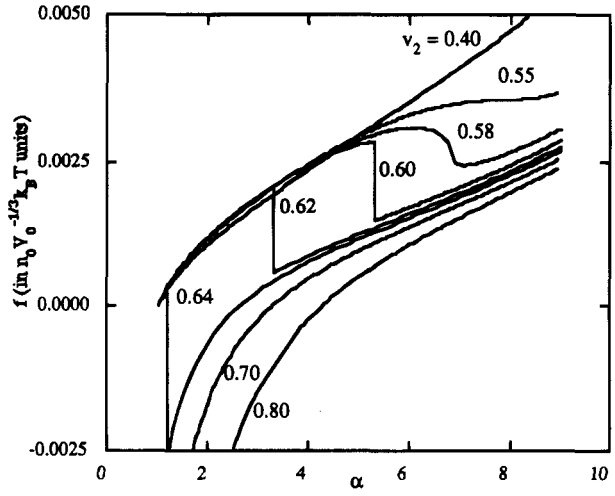

Figure 3. Force f versus extension ratio α_d for a swollen network undergoing phase transitions at constant length.

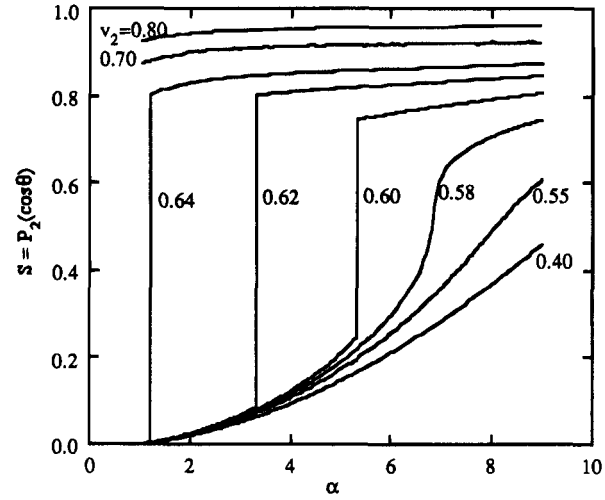

Figure 4. Orientation function S versus extension ratio α_e for a swollen network undergoing phase transitions at constant length.

equal to 0.40 (within the range of extensions studied), and the network is always isotropic. For networks with high values of v_2 (0.70 and 0.80), the f–α_e relation characteristic of the nematic phase is always displayed, even around $\alpha_e \cong 1$, suggesting that the concentration of the polymer is above the critical value v_{2c}, and thus even the undeformed network is nematic. It should be noted that Figure 2 shows that for $v_2 > 0.62$ at $f = 0$ the network exhibits an $\alpha > 1$. This is due to the symmetry-breaking of the solutions of the model implied by the choice of the direction of the stress. The solution $f = 0$ corresponds to the limit $f \to 0$. In the experiments performed without external fields a polydomain sample exists with overall dimensions of the isotropic system. Figure 3 shows that for $v_2 > 0.62$ the transition at constant length leads to a compression force ($f < 0$) implied by the fixed direction (parallel to the stress axis) of the director. However, under real experimental conditions, one may obtain reorientation of the director of the sample instead of the compression.

The orientation function S for the same network ($x = 12$, $m = 100$) during the phase transitions at constant length is shown in Figure 4. The results are presented as a function of the extension ratio α_e for varying values of the volume fraction of the polymer. For v_2 equal to 0.40 and 0.55, S is relatively small and shows no discontinuity, which suggests that the network remains

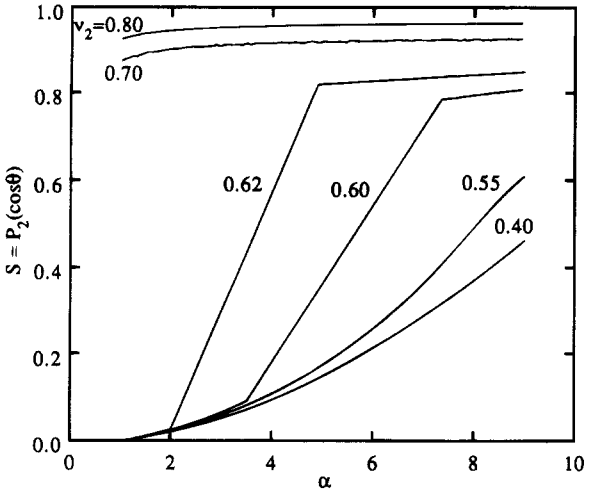

Figure 5. Orientation function S versus extension ratio α_e for a swollen network undergoing phase transitions at constant force.

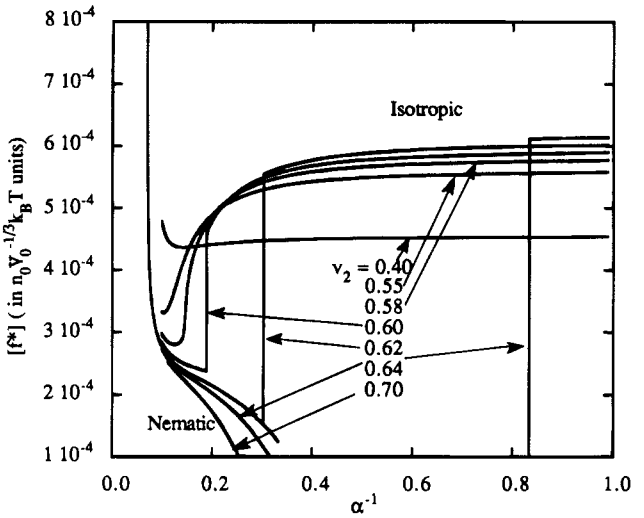

Figure 6. Reduced modulus $[f^*]$ versus inverse elongation α_e^{-1} with phase transitions at constant length.

isotropic during the extension. The abrupt increase in S for networks with v_2 from 0.58 to 0.62 is the indication of a strain-induced transformation from the isotropic to the nematic state at constant length. The nematic state is far more ordered than the isotropic phase and thus has a much higher orientation parameter S. The very large values of S for networks with v_2 equal to 0.70 and 0.80 and at $\alpha_e = 1$ show that these networks have volume fractions of polymer above the critical value v_{2c} and, therefore, always exist in the highly-ordered nematic state. Figure 4 shows that there is a critical concentration $v_2 \approx 0.58$, where the isotropic–nematic transition becomes continuous. For concentrations of the polymer $v_2 > 0.58$ the transition is of the first order, for $v_2 < 0.58$ it becomes of the second order, and for smaller values of v_2 the isotropic–nematic transition disappears. The existence of such critical points has been predicted by de Gennes.[41] Similar results are shown in Figure 5 for phase transitions occurring at constant force. The discontinuities of the $S-\alpha_e$ curves during the phase transition in Figure 5 involve abrupt changes not only in S but also in α_e.

Figures 6 and 7 show the reduced modulus $[f^*]$ as a function of reciprocal elongation α_e^{-1} for varying values of v_2. Figure 6 corresponds to phase transitions at constant length, while Figure 7 illustrates the case of

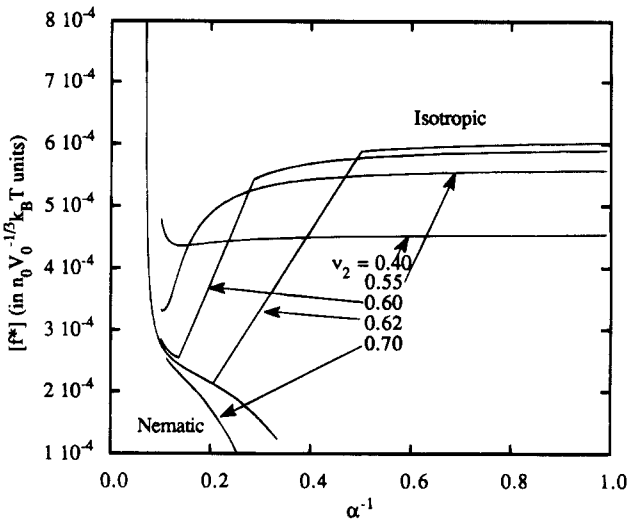

Figure 7. Reduced modulus $[f^*]$ versus inverse elongation α_e^{-1} for a swollen network undergoing phase transitions at constant force.

phase transitions at constant force. An isotropic network with $v_2 = 0.40$ displays a constant reduced modulus $[f^*]$, regardless of the elongation (up to large elongations, where the effect of the limited chain extensibility starts playing a role), resembling the affinely-deformed Gaussian chain network. For the nematic network with high values of v_2 (0.70), $[f^*]$ decreases with an increase in α_e^{-1}. Both curves for $v_2 = 0.40$ (isotropic phase) and 0.70 (nematic phase) exhibit continuity in the $[f^*]-\alpha_e^{-1}$ relation due to limited chain extensibility, without occurrence of a phase transformation. The network with v_2 around 0.60 shows extraordinary stress–strain behavior. At small elongations before the phase transition point, the network is isotropic and the modulus $[f^*]$ is constant. During the phase transition, $[f^*]$ drops sharply and the curve passes from the isotropic branch to the nematic branch. Finally, it increases with an increase in α_e (a decrease in α_e^{-1}) in a way similar to that for the nematic network ($v_2 = 0.70$). This theoretically predicted behavior of the modulus $[f^*]$ was experimentally observed for strain-induced crystallization of some rubbery materials.[1] The downturn followed by upturn in $[f^*]$ calculated here is obviously associated with the strain-induced liquid-crystalline isotropic–nematic phase transformation in the stretched semirigid chain network.

The birefringence Δn (normalized by Δn_0) for uniaxially-deformed networks as a function of true stress σ is shown in Figures 8 and 9. Figure 8 illustrates the case of the isotropic–nematic phase transitions occurring at constant length, while Figure 9 corresponds to the case at constant stress. The behavior of Δn as a function of the true stress σ is quite similar to that of the orientation parameter S with respect to the extension α_e. The discontinuities again occur at the strain-induced isotropic–nematic phase transition points. Figure 8 shows a slight decrease in stress during the phase transition at constant length. The phase transition at constant force (as seen in Figure 2) is accompanied by a large increase in the length of the sample. For a transition at fixed length, the sample has to be compressed, which results in a decrease in stress. Under experimental conditions, instead of the compression, there could be reorientation of the director of the sample.

Figure 10 shows a plot of the reduced birefringence $[\Delta n]$ (normalized by Δn_0) versus reciprocal elongation

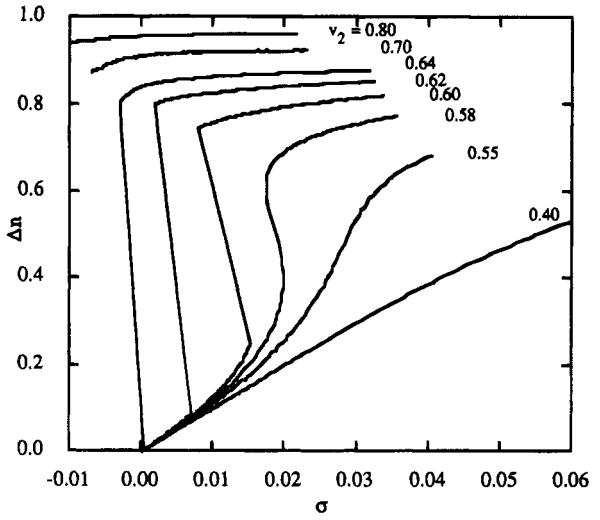

Figure 8. Birefringence versus true stress σ for a swollen network undergoing phase transitions at constant length.

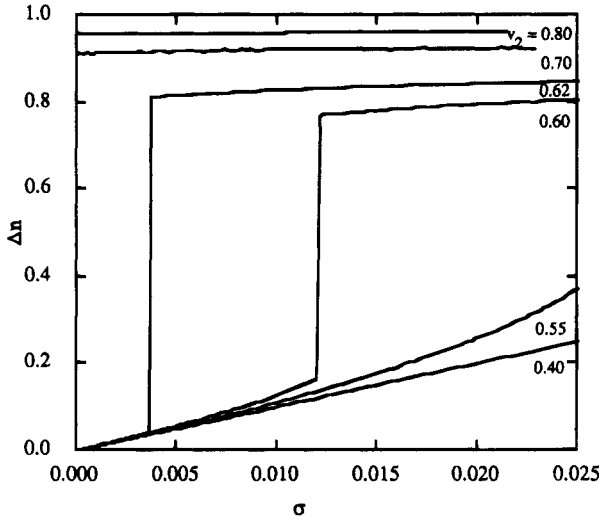

Figure 9. Birefringence versus true stress σ for a swollen network undergoing phase transitions at constant force.

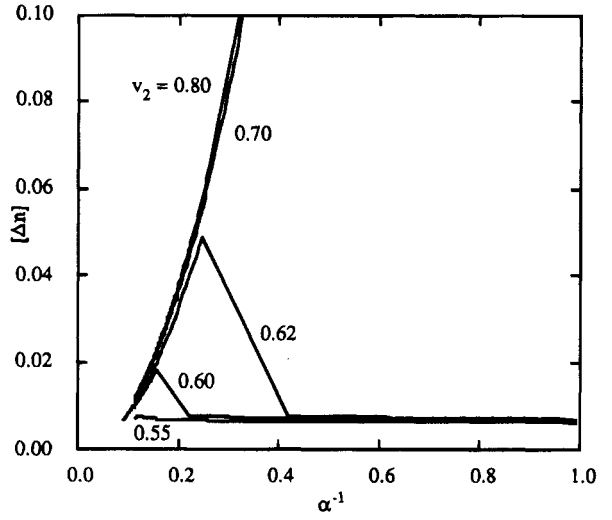

Figure 10. Reduced birefringence versus inverse elongation α_e^{-1} for a swollen network undergoing phase transitions at constant stress.

α_e^{-1}, for phase transitions at constant stress. The isotropic network with $v_2 = 0.55$ exhibits the strain-optical behavior of the affine model, for which the reduced birefringence is constant during extension. For

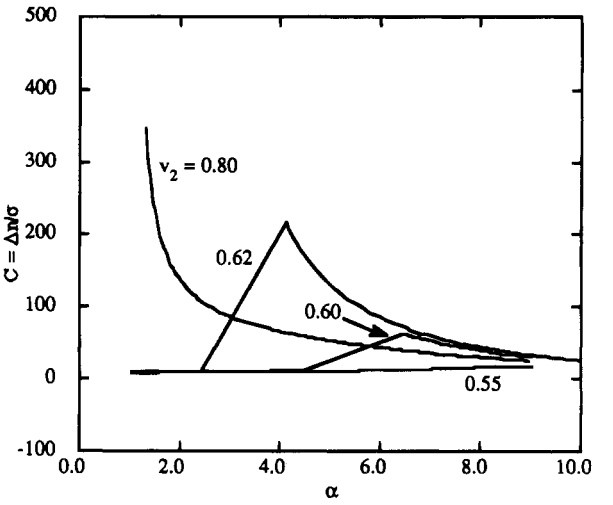

Figure 11. Stress-optical coefficient C in units of $(n_0V_0^{-1/3}k_BT)^{-1}$ versus elongation α_e for a swollen network undergoing phase transitions at constant stress.

swollen networks with v_2 equal to 0.60 and 0.62, the isotropic phase is observed at small elongations, where $[\Delta n]$ remains unchanged. Once a transition point is reached, $[\Delta n]$ drastically increases with extension during the phase transition. It finally decreases with elongation when a nematic phase is reached. For nematic networks (v_2 = 0.7 and 0.8) a monotonic decrease of $[\Delta n]$ with an increase of α_e is always observed.

The stress-optical coefficient C is plotted versus the extension α_e in Figure 11, for the case of phase transitions occurring at constant stress. The stress-optical coefficient C is again constant for an isotropic network at $v_2 = 0.40$. The discontinuities in C for v_2 equal to 0.60 and 0.62 are due to the isotropic-to-nematic phase transformation. For the network with $v_2 = 0.80$, the stress-optical coefficient C approaches infinity when α_e is close to 1, because the network is in a highly-ordered nematic state with the orientation function S almost equal to 1, even for the undeformed polymer. It decreases dramatically with an increase of extension and finally reaches a steady value.

Conclusions

The above theoretical treatment clarifies the molecular origin of the discontinuities in stress–strain and stress-optical birefringence relationships associated with isotropic–nematic transition phenomena in swollen networks of semirigid chains. In particular, the present model rationalizes several experimental observations such as the abrupt change in the dimensions of liquid-crystalline networks subject to uniaxial deformation at constant force, the sharp minimum in the modulus as a function of the extension ratio, and discontinuities in the order parameter and the optical birefringence revealed by optical methods during deformation. The model has been developed for lyotropic liquid-crystalline networks, but it may easily be refined to include thermotropic effects as well. The basic predictions of the model agree with the results of the theory of Warner developed for thermotropic liquid crystals and based on the wormlike chain model.[27,28]

An interesting feature of the theory is the observation that phase transitions may be induced in stretched swollen networks upon deswelling of the material. This calls attention to a novel technique being developed for producing highly-oriented material by stretching a

network in the swollen state, with subsequent removal of the solvent in the strained state.[47,48]

Acknowledgment. It is a pleasure to acknowledge the financial support provided by Procter & Gamble Co. through a University Exploratory Research Program Grant and by the National Science Foundation through Grant DMR 89-18002 (Polymers Program, Division of Materials Research).

References and Notes

(1) Mark, J. E.; Erman, B. *Rubberlike Elasticity. A Molecular Primer*; Wiley-Interscience: New York, 1988.
(2) Treloar, L. R. G. *The Physics of Rubber Elasticity*, 3rd ed.; Clarendon Press: Oxford, U.K., 1975.
(3) Erman, B.; Mark, J. E. *Annu. Rev. Phys. Chem.* **1989**, *40*, 351.
(4) Queslel, J. P.; Mark, J. E. In *Encyclopedia of Polymer Science and Engineering*, 2nd ed.; Mark, H. F., Bikales, N. M., Overberger, C. G., Menges, G., Kroschwitz, J. I., Eds.; John Wiley & Sons: New York, 1986; Vol. 5.
(5) Erman, B. In *Encyclopedia of Polymer Science and Engineering*, 2nd ed.; Supplement, Mark, H. F., Bikales, N. M., Overberger, C. G., Menges, G., Kroschwitz, J. I., Eds.; John Wiley & Sons: New York, 1986.
(6) Flory, P. J.; Erman, B. *Macromolecules* **1982**, *15*, 800.
(7) Erman, B.; Flory, P. J. *Macromolecules* **1982**, *15*, 806.
(8) Erman, B.; Monnerie, L. *Macromolecules* **1989**, *22*, 3342.
(9) Erman, B.; Flory, P. J. *Macromolecules* **1983**, *16*, 1601, 1607.
(10) Erman, B.; Bahar, I.; Yang, Y.; Kloczkowski, A.; Mark, J. E. In *Polymer Solutions, Blends, and Interfaces*; Noda, I., Rubingh, D. N., Eds.; Elsevier Science: Amsterdam, The Netherlands, 1992.
(11) Reference 11, to be added.
(12) Finkelmann, H.; Kock, H.-J.; Rehage, G. *Makromol. Chem., Rapid Commun.* **1981**, *2*, 317.
(13) Finkelmann, H.; Rehage, G. *Makromol. Chem., Rapid Commun.* **1982**, *3*, 859.
(14) Hanus, K.-H.; Pechhold, W.; Soergel, F.; Stoll, B.; Zental, R. *Colloid Polym. Sci.* **1990**, *268*, 222.
(15) Zental, R.; Reckert, G. *Makromol. Chem.* **1986**, *187*, 1915.
(16) Schätzle, J.; Kaufhold, W.; Finkelmann, H. *Makromol. Chem.* **1989**, *190*, 3269.
(17) Bualek, S.; Zental, R. *Makromol. Chem.* **1988**, *189*, 791.
(18) Finkelmann, H.; Kock, H.-J.; Gleim, W.; Rehage, G. *Makromol. Chem., Rapid Commun.* **1984**, *5*, 287.
(19) Schätzle, J.; Finkelmann, H. *Mol. Cryst. Liq. Cryst.* **1987**, *142*, 85.
(20) Zental, R.; Benalia, M. *Makromol. Chem.* **1987**, *188*, 665.
(21) Mitchell, G. R.; Davis, F. J.; Ashman, A. *Polymer* **1987**, *28*, 639.
(22) Bualek, S.; Kapitza, H.; Mayer, J.; Schmidt, G. F.; Zental, R. *Mol. Cryst. Liq. Cryst.* **1988**, *155*, 47.
(23) Zental, R.; Rerkert, G.; Bualek, S.; Kapitza, K. *Makromol. Chem.* **1989**, *190*, 2869.
(24) Löffler, R.; Finkelmann, H. *Makromol. Chem., Rapid Commun.* **1989**, *11*, 321.
(25) Endres, A. W.; Wendorff, J. H. *Makromol. Chem.* **1987**, *188*, 1501.
(26) Warner, M.; Gelling, K. P.; Vilgis, T. A. *J. Chem. Phys.* **1988**, *88*, 4008.
(27) Warner, M.; Wang, X. J. *Macromolecules* **1991**, *24*, 4923.
(28) Warner, M.; Wang, X. J. In *Elastomeric Polymer Networks*; Mark, J. E., Erman, B., Eds.; Prentice Hall: Englewood Cliffs, NJ, 1992.
(29) Erman, B.; Bahar, I.; Kloczkowski, A.; Mark, J. E. *Macromolecules* **1991**, *23*, 5335.
(30) Bahar, I.; Erman, B.; Kloczkowski, A.; Mark, J. E. *Macromolecules* **1991**, *23*, 5347.
(31) Erman, B.; Bahar, I.; Kloczkowski, A.; Mark, J. E. In *Elastomeric Polymer Networks*; Mark, J. E., Erman, B., Eds.; Prentice Hall: Englewood Cliffs, NJ, 1992.
(32) Suto, S.; Tashiro, H. *Polymer* **1989**, *30*, 2063.
(33) Suto, S.; Tashiro, H.; Karasawa, M. *J. Appl. Polym. Sci.* **1992**, *45*, 1569.
(34) Suto, S. *J. Appl. Polym. Sci.* **1989**, *37*, 2781.
(35) Song, C. Q.; Litt, M. H.; M-Zloczower, I. *J. Appl. Polym. Sci.* **1991**, *42*, 2517.
(36) Song, C. Q.; Litt, M. H.; M-Zloczower, I. *Macromolecules* **1992**, *25*, 2166.
(37) Aharoni, S. M.; Edwards, S. F. *Macromolecules* **1989**, *22*, 3361.
(38) Hatfield, R.; O'Brien, K. P.; Aharoni, S. M. *Macromolecules* **1990**, *23*, 1330.
(39) Yang, Y.; Kloczkowski, A.; Mark, J. E.; Erman, B.; Bahar, I. **1995**, *28*, 4927.
(40) de Gennes, P.-G. *The Physics of Liquid Crystals*; Clarendon Press: Oxford, U.K., 1974.
(41) de Gennes, P.-G. In *Polymer Liquid Crystals*; Ciferri, A., Krigbaum, W. R., Mayer, R. B., Eds.; Academic Press: New York, 1982.
(42) Flory, P. J.; Ronca, G. *Mol. Cryst. Liq. Cryst.* **1979**, *54*, 289, 311.
(43) Flory, P. J. In *Advances in Polymer Science*; Gordon, M., Platé, N. A., Eds.; Springer-Verlag: Berlin, 1984; Vol. 59.
(44) Kloczkowski, A.; Mark, J. E.; Erman, B.; Bahar, I. In *Polymer Solutions, Blends, and Interfaces*; Noda, I., Rubingh, D. N., Eds.; Elsevier Science: Amsterdam, The Netherlands, 1992.
(45) Hermans, P. H. *Contribution to the Physics of Cellulose Fibres*; Elsevier: New York, 1940.
(46) Volkenstein, M. V. *Configurational Statistics of Polymeric Chains*; Interscience: New York, 1963.
(47) Yang, Y.; Kloczkowski, A.; Mark, J. E.; Erman, B.; Bahar, I. *Colloid Polym. Sci.*, in press.
(48) Mark, J. E.; Yang, Y.; Kloczkowski, A.; Erman, B.; Bahar, I. *Colloid Polym. Sci.*, in press.

MA9462262